Room-temperature ferromagnetic Co-doped ZnO nanoneedle array prepared by pulsed laser deposition

J. J. Chen, M. H. Yu, and W. L. Zhou[a)]
Advanced Materials Research Institute, University of New Orleans, New Orleans, Louisiana 70148

K. Sun and L. M. Wang
Department of Nuclear Engineering and Radiological Sciences, University of Michigan, Ann Arbor, Michigan 48109

(Received 4 April 2005; accepted 1 September 2005; published online 20 October 2005)

A Co-doped ZnO nanoneedle array with room-temperature ferromagnetic properties was successfully fabricated by pulsed laser deposition (PLD) method. Detailed nanostructures were studied by transmission electron microscopy (TEM) and x-ray diffraction (XRD). High resolution TEM images and selected area electron diffraction (SAD) patterns showed nanoneedles grew along *c*-axis of ZnO with a preferential growth perpendicular to Si (100) substrate, which is also confirmed by XRD. Uneven surface and stacking faults along the nanoneedles were observed, which implies lattice distortion due to the Co doping. Electron energy loss spectroscopy (EELS) analysis of different positions along the growth direction of nanoneedles shows homogeneous distribution of the Co dopant. No segregated clusters of impurity phase were detected by TEM. Superconducting quantum interference device (SQUID) magnetometer measurements show room temperature ferromagnetic ordering, which is attributed to the Co substitution for Zn in the ZnO nanoneedle. [DOI: 10.1063/1.2119415]

In recent years, diluted magnetic semiconductors (DMSs) have stimulated much interest because of their promising applications in spintronic devices, such as spin-valve transistors, spin light-emitting diodes, nonvolatile memory, etc.[1,2] Therefore, ferromagnetic DMSs with Curie temperature (T_C) higher than room temperature are crucial for practical device applications. Dietl *et al.*[3] theoretically predicted that ZnO-based DMSs probably have room-temperature ferromagnetism, initiating intensive research on ZnO doped with different 3*d* transition metals (Co, Mn, Fe, Ni, Cr, etc). Following the original research by Ueda *et al.*,[4] many reports[5–8] have been given about Co-doped ZnO thin films exhibiting ferromagnetism with T_C above room-temperature.

On the other hand, synthesis of one-dimensional ZnO nanostructures doped with 3*d* transition metals also attracts much attention for their potential applications in spintronic nanodevices. ZnO nanowires and nanorods doped with 3*d* transition metals were fabricated by different groups;[9–14] however, few groups presented one-dimensional doped ZnO with ferromagnetic ordering above the room temperature. Wu *et al.*[9] demonstrated the growth of well-aligned $Zn_{1-x}Co_xO$ nanorods using chemical vapor deposition (CVD) methods and achieved room temperature ferromagnetic ordering. Pearton *et al.*[10] implanted Mn ions and Co ions into the catalyst-driven ZnO nanorods, and for both types of implanted dopants, the ferromagnetism persisted to temperatures of 225–300 K. In this letter, synthesis of a Co-doped ZnO nanoneedle array with room temperature ferromagnetic ordering using pulsed laser deposition (PLD) method is presented.

Co-doped ZnO nanoneedles were formed on silicon (100) substrate by PLD. A sintered $Zn_{0.95}Co_{0.05}O$ target was prepared using the standard ceramic technique. The neodymium-doped yttrium aluminum garnet (Nd:YAG) laser was used to evaporate the target materials. The laser wavelength, energy density, and pulse frequency were 266 nm, 2 J/cm^2, and 2 Hz, respectively. Before the deposition, the vacuum system was pumped to 1×10^{-3} Torr, and 20 mTorr oxygen partial pressure was used. The silicon substrate was maintained at 750 °C during the deposition, and the target-substrate distance was 45 mm. The total deposition duration was 180 min. The morphology of as-synthesized $Zn_{0.95}Co_{0.05}O$ nanoneedles was investigated by Carl Zeiss 1530 VP field-emission scanning electron microscope (FESEM). Nanostructures of the nanoneedles were determined by JEOL 2010 transmission electron microscope (TEM) equipped with EDAX DXPrime electron energy dispersive x-ray analysis (EDS). Electron energy loss spectroscopy (EELS) and energy filter TEM (EFTEM) were obtained using a JEOL 2010F STEM/TEM equipped with Gatan imaging filter (GIF). X-ray diffraction (XRD) θ-2θ and ω scan were done by Philips X'Pert MPD using a Cu $K\alpha$ source. The magnetic properties of the samples were measured by Quantum Design MPMS-5S superconducting quantum interference device (SQUID) magnetometer.

Figure 1 shows a typical FESEM image of the Co-doped ZnO nanoneedles. The nanoneedles had a growth direction preferentially perpendicular to Si substrate and formed over the whole substrate. Figure 2(a) is a high-resolution electron microscopy (HREM) image of the ZnO nanoneedle along the $[2\bar{1}\bar{1}0]$ zone axis. No catalyst particles were found at the tip of nanoneedles, suggesting catalyst-free growth mechanism. The enlarged image, highlighted by the upper rectangular area of Fig. 2(a), shows that the nanoneedle grew along the *c*-axis of the wurtzite ZnO structure [Fig. 2(b)]. The inset of Fig. 2(b) is the corresponding selected area electron diffraction (SAD) pattern, which confirms *c*-axis growth of the nanoneedle. However, an uneven surface and a number of

a)Author to whom correspondence should be addressed; electronic mail: wzhou@uno.edu

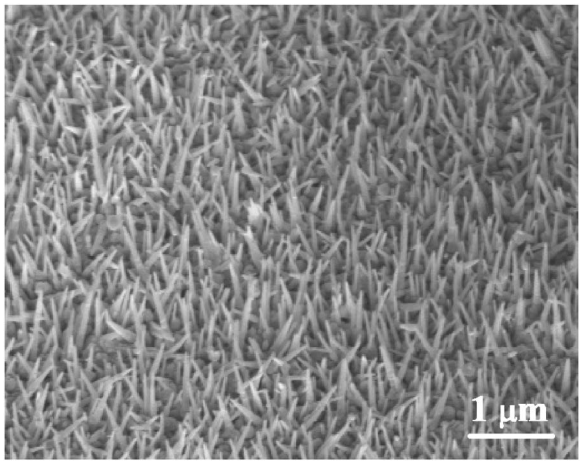

FIG. 1. FESEM image of Co-doped ZnO nanoneedle array. The average diameter of the bottom of the nanoneedles is about 60 nm and the average length is about 300 nm.

stacking faults were seen along the nanoneedles. A representative surface structure with stacking faults [the lower rectangular area of Fig. 2(a)] is shown in Fig. 2(c), and its back and forth fast Fourier transformation (FFT) image using the 000 ± 1 diffraction spots is displayed in Fig. 2(d).[13] Two edge dislocations (denoted by arrows) associated with the stacking faults were clearly observed. These lattice defects might be attributed to the stress introduced by substitution of Co ions for the Zn sites in the ZnO lattice. It might also cause the uneven surface of the nanoneedle. Furthermore, no segregated clusters of impurity phase were detected.

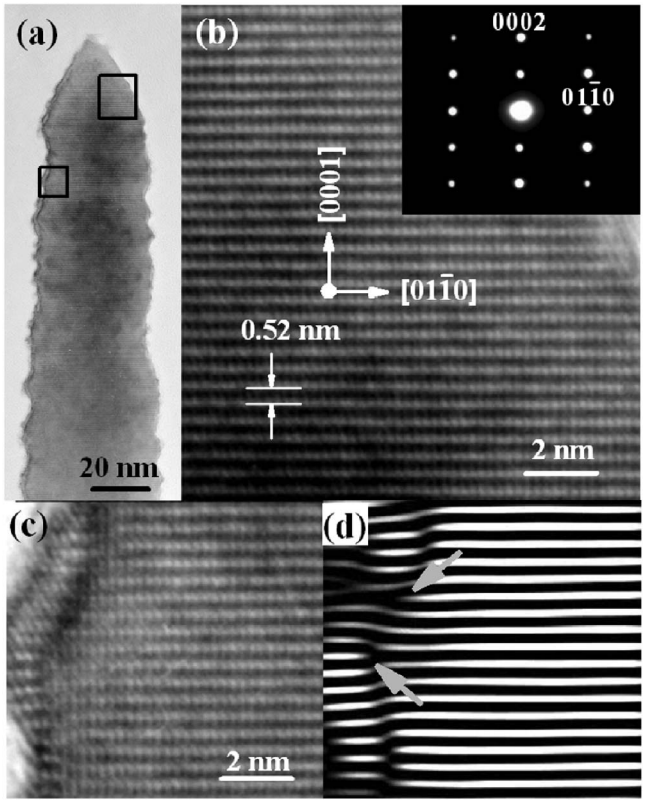

FIG. 2. (a) TEM image of a Co-doped ZnO nanoneedle. (b) HREM image of upper rectangular area and corresponding SAD pattern (inset), showing *c*-axis growth. (c) HREM image of lower rectangular area, showing typical stacking faults near the nanoneedle surface. (d) The back and forth fast Fourier transformation (FFT) image of (c) by using the 000 ± 1 spots. Two edge dislocations associated with the stacking faults is denoted by arrows.

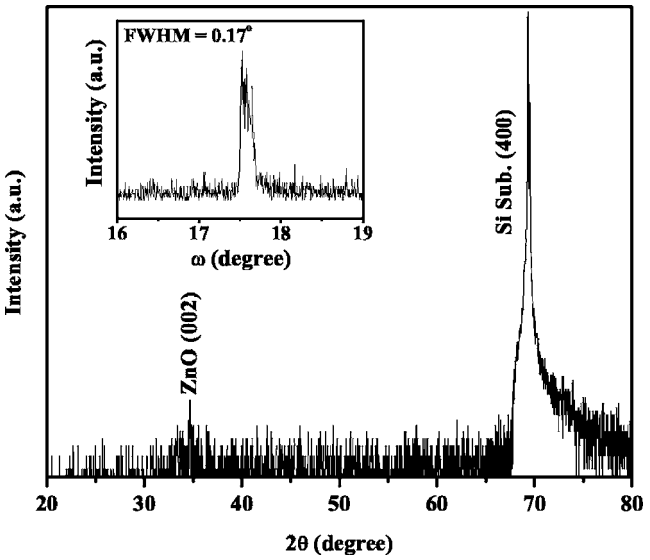

FIG. 3. XRD θ-2θ pattern of Co-doped ZnO nanoneedles on Si (100) substrate. The rocking curve (ω-scan) on ZnO (002) reflection is also shown (inset), which confirms the *c*-axis dominated growth.

In the XRD θ-2θ scan, as illustrated in Fig. 3, only ZnO (002) and Si (400) reflections were detected, which confirmed *c*-axis dominated nanoneedle growth. The inset is XRD rocking curve (ω-scan) on the ZnO (002) reflection. The full-width-half-maximum (FWHM) of this peak is about 0.17°, which demonstrates *c*-axis preferential growth of the nanoneedles.

In order to confirm substitution of Co ions for Zn in the lattice, electron energy loss spectroscopy (EELS) was employed. By positioning the nanoprobe along *c*-axis of a nanoneedle [Fig. 4(a)], Co $L_{2,3}$ peaks with similar intensity were obtained as shown in Fig. 4(b). EELS mapping observation also shows that cobalt homogeneously distributes along the nanoneedles. EDS collected on various points shows the average concentration of Co is about 4.6 at %, in good agreement with the target composition of 5 at %.

Figure 5 is the hysteresis loop of the nanoneedle array at 300 K. The sample exhibits room temperature ferromagnetism with coercivity of about 90 Oe and the saturation magnetization of about 0.08 μ_B/Co. For the low temperature

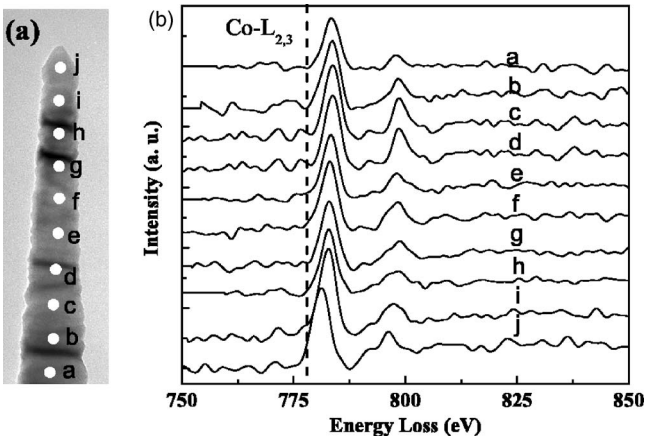

FIG. 4. (a) TEM image showing the probe positions along the growth direction of the nanoneedle for EELS measurement and (b) corresponding EELS spectra. The Co-$L_{2,3}$ edge is shown by the dashed line.

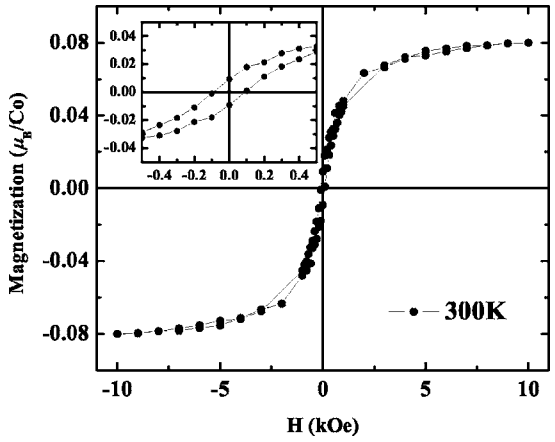

FIG. 5. Hysteresis loop of $Zn_{0.95}Co_{0.05}O$ nanoneedles at room temperature, and inset image show the enlargement of the hysteresis loop. The coercivity is about 90 Oe and the saturation magnetization is 0.08 μ_B/Co. Data are corrected for the diamagnetism of the Si substrate.

SQUID measurement, the coercivity and the saturation magnetization increased to 120 Oe and 0.34 μ_B/Co at 5 K. This room temperature ferromagnetism is attributed to successfully doping Co in the ZnO nanoneedles.

In summary, a Co-doped ZnO nanoneedle array was fabricated on a silicon substrate by PLD method. HREM and XRD results showed that the nanoneedles grew along the *c*-axis with a preferential alignment perpendicular to the substrate. EELS analysis clearly demonstrated the homogeneous distribution of Co along ZnO nanoneedles. Room temperature ferromagnetism was achieved, which is attributed to the successfully doping of Co into the ZnO nanoneedles.

This work was supported by the DARPA Grant No. HR0011-04-1-0029 and a research grant from Louisiana Board of Regents Contract No. LEQSF (2003-06)-RD-B-13. The authors gratefully acknowledge Dr. Zhenjun Wang for helping to obtain the XRD results.

[1] J. K. Furdyna, J. Appl. Phys. **64**, R29 (1988).
[2] S. J. Pearton, W. H. Heo, M. Ivill, D. P. Norton, and T. Steiner, Semicond. Sci. Technol. **19**, R59 (2004).
[3] T. Dietl, H. Ohno, F. Matsukura, J. Cibert, and D. Ferrand, Science **287**, 1019 (2000).
[4] K. Ueda, H. Tabata, and T. Kawai, Appl. Phys. Lett. **79**, 988 (2001).
[5] H. J. Lee, S. Y. Jeong, C. R. Cho, and C. H. Park, Appl. Phys. Lett. **81**, 4020 (2002).
[6] W. Prellier, A. Fouchet, B. Mercey, Ch. Simon, and B. Raveau, Appl. Phys. Lett. **82**, 3490 (2003).
[7] D. P. Norton, M. E. Overberg, S. J. Pearton, K. Pruessner, J. D. Budai, L. A. Boatner, M. F. Chisholm, J. S. Lee, Z. G. Khim, Y. D. Park, and R. G. Wilson, Appl. Phys. Lett. **83**, 5488 (2003).
[8] M. Venkatesan, C. B. Fitzgerald, J. G. Lunney, and J. M. D. Coey, Phys. Rev. Lett. **93**, 177206 (2004).
[9] J. J. Wu, S. C. Liu, and M. H. Yang, Appl. Phys. Lett. **85**, 1027 (2004).
[10] K. Ip, R. M. Frazier, Y. W. Heo, D. P. Norton, C. R. Abernathy, S. J. Pearton, J. Kelly, R. Rairigh, A. F. Hebard, J. M. Zavada, and R. G. Wilson, J. Vac. Sci. Technol. B **21**, 1476 (2003).
[11] Y. Q. Chang, D. B. Wang, X. H. Luo, X. Y. Xu, X. H. Chen, L. Li, C. P. Chen, R. M. Wang, J. Xu, and D. P. Xu, Appl. Phys. Lett. **83**, 4020 (2003).
[12] V. A. Roy, A. B. Djurisic, H. Liu, X. X. Zhang, Y. H. Leung, M. H. Xie, J. Gao, H. F. Lui, and C. Surya, Appl. Phys. Lett. **84**, 756 (2004).
[13] C. Ronning, P. X. Gao, Y. Ding, Z. L. Wang, and D. Schwen, Appl. Phys. Lett. **84**, 783 (2004).
[14] R. K. Zheng, H. Liu, X. X. Zhang, V. A. L. Roy, and A. B. Djurisic, Appl. Phys. Lett. **85**, 2589 (2004).